Energy budget diagnosis of changing climate feedback

B. B. Cael[1,*], Jonah Bloch-Johnson[2], Paulo Ceppi[3], Hege-Beate Fredriksen[4],

Philip Goodwin[5], Jonathan Gregory[2,6], Christopher J. Smith[7,8], and Richard G. Williams[9]

1. National Oceanography Centre, Southampton, UK. 2. National Centre for Atmospheric Science, Reading, UK. 3. Imperial College London, UK. 4. UiT The Arctic University of Norway, Tromsø, Norway. 5. University of Southampton, UK. 6. Met Office Hadley Centre, Exeter, UK. 7. University of Leeds, UK. 8. International Institute for Applied Systems Analysis, Laxenburg, Austria. 9. University of Liverpool, UK.

*cael@noc.ac.uk.

This paper is a non-peer reviewed preprint submitted to EarthArXiv.

Short title: Observed climate feedback change

One-Sentence Summary: Records of Earth's energy budget indicate that Earth's climate feedback has changed substantially over the past 50 years.

Keywords: Climate change; climate feedback; pattern effect; radiative forcing; ocean heat content; climate modelling

---

Abstract

The climate feedback determines how Earth's climate responds to anthropogenic forcing. It has been more negative in recent decades than predicted by Earth system models due to a sea surface temperature 'pattern effect', whereby warming is concentrated in the western tropical Pacific, where nonlocal radiative feedbacks are very negative. This phenomenon has however primarily been studied within climate models. We diagnose a pattern effect from historical records as an evolution of the climate feedback over the past five decades. The climate feedback has decreased by 0.8 ± 0.5 W/m^{2}K over the past 50 years, corresponding to a reduction in climate sensitivity. Earth system models' climate feedbacks instead increase over this period. Understanding and simulating this historical trend and its future evolution are critical for reliable climate projections.

Earth's climate feedback – the amount of extra energy radiated to space per degree of global warming ($-\lambda$, [W/m^{2}K]) – is a central object of study in climate science, being one of the essential parameters determining Earth's response to anthropogenic emissions of greenhouse gases and other forcing agents [1]. If λ is more negative, Earth's global mean surface temperature T [K] is less sensitive to the anthropogenic radiative forcing F [W/m^2], i.e. $-\lambda$ is inversely proportional to effective climate sensitivity (defined as the projected equilibrium warming following a doubling of the preindustrial CO_2 concentration) [2]. Though myriad physical processes contribute to λ, a crucial factor is the spatial pattern of warming. In particular, warming in the western tropical Pacific produces a much larger global radiative response, and hence a more negative climate feedback, than warming elsewhere; this phenomenon has been termed the 'pattern effect' [3, 4, 5, 6, 7]. Warming in this region, where air moves upwards in the lower atmosphere, results in increased stability of the lower tropical atmosphere in remote subsidence regions; this in turn increases low cloud cover and hence upwards shortwave radiation. In recent decades, global warming has been concentrated in this region of very negative radiative feedbacks [8, 9, 4, 10], leading to a more negative value of λ (hence lower climate sensitivity).

When simulating the historical climate over recent decades, Earth system models (ESMs) tend to produce spatial warming patterns that lack this concentration of warming in regions of very negative radiative feedbacks. The ESM projections lead to less negative λ (higher climate sensitivity) than when the observed spatial pattern of sea surface temperature is imposed on the same atmospheric models [11]. Furthermore, for standard ESM simulations with fixed atmospheric CO_2 concentrations quadrupling from preindustrial levels – the primary model experiment for diagnosing the global climate feedback λ – the spatial pattern of warming is again quite different, leading to a less negative λ than indicated by observations [12]. The pattern effect is thus sometimes quantified by the difference between the λ values associated with a CO_2-quadrupling experiment and an experiment with prescribed sea surface temperatures [9], based on the argument that the surface warming should eventually adjust to the modelled long-term warming pattern. The pattern effect quantified as such has been almost exclusively studied within ESMs because we cannot instantaneously quadruple the atmospheric CO_2 concentration.

It would be advantageous to quantify a pattern effect from historical records, not only to assess the probability, magnitude, and implications of this effect for Earth's recent climate, but also to provide a benchmark with which to assess ESM performance. This observationally-based viewpoint is especially important because it is increasingly common to weight models in multi-model projections by their relative performance in capturing historical trends, which they may do for the wrong reasons, thereby biasing projections, if they do not capture the influence of the pattern effect [13, 14, 15, 16].

Here we propose an alternative metric for the pattern effect – the *trend* in the climate feedback λ over recent decades – that can be diagnosed from historical records without reference to hypothetical scenarios. We show that this trend is significantly different from zero over the past five decades of global energy budget records, and large in amplitude with substantial implications for global warming. We also show that ESMs fail to capture this trend, irrespective of their climate sensitivity. We use the past five decades because this is the time period over which reliable records exist [17] (Methods). The bulk of global warming has occurred since 1970, with four of the first six years of the 1970s being within 0.2°C of the 1850–1900 average [18], as has the bulk of the increase in ocean heat content $\mathcal{H}$ [W yr/m^2] and radiative forcing [17, 19]. We stress from the outset that we only investigate this period of 1970–2019; we make no assumptions or speculations about the future trends in λ, though the pattern effect is generally expected to reverse in future, whether due to adjustment of the warming pattern to the radiative forcing over a multidecadal timescale, or to future changes in radiative forcing patterns.

The method we present is described in detail in the Methods. Briefly, we work from a simple Earth energy balance equation, which states that the rate of global warming is proportional to the net rate of energy storage in the upper ocean

$$\eta \dot{T}(t) = F(t) + \lambda(t)T(t) - H(t), \tag{1}$$

where T [K] is the global mean surface temperature anomaly, η [W yr/m^{2}K] is the heat capacity of the upper ocean layer, F [W/m^2] is the radiative forcing imposed upon Earth's surface, λ [W/m^{2}K] is the climate feedback, and H [W/m^2] is the ocean heat uptake (the flux of energy into the deeper ocean from the upper layer). From this equation one can derive the energy budget $\mathcal{F}(\tau) - \mathcal{H}(\tau) = \mathcal{R}(\tau)$, where $\mathcal{F}(\tau)$ is the cumulative energy fluxed to the top of the atmosphere via radiative forcing by time τ, $\mathcal{H}(\tau)$ is the total ocean heat content anomaly at time τ (including the upper layer), which approximates the Earth's energy imbalance, and $\mathcal{R}(\tau)$ is the cumulative energy fluxed back to space by

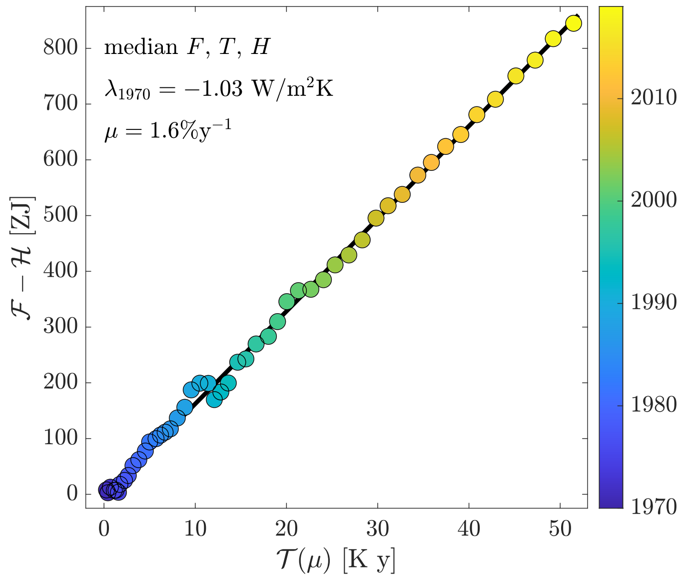

Figure 1: Illustration of diagnosis of model parameters from time series, using the medians of radiative forcing, ocean heat content, and global mean surface temperature; see Methods for details. x-axis is the weighted temperature anomaly integral; y-axis is the cumulative anomaly in energy radiated to space ($\mathcal{F} - \mathcal{H}$); color is year.

time τ; this is just a restatement of conservation of energy. We then make the ansatz that λ changes linearly with time from 1970, i.e. $\lambda(t) = \lambda_{1970}(1 + \mu t)$ where t is time in years since 1970. This choice is motivated by its simplicity as a means to capture the expected change in λ from 1970–2019 as warming concentrated in the western tropical Pacific, and is justified post hoc by the absence of systematic behavior in the residuals (Methods). Substituting this ansatz into the energy budget yields

$$\mathcal{F}(\tau) - \mathcal{H}(\tau) = -\lambda_{1970}\mathcal{T}(\mu, \tau), \tag{2}$$

where $\mathcal{T}(\mu, \tau)$ is a weighted integral of the temperature anomaly (Methods). The parameter combinations (λ_{1970}, μ) that minimize the residuals of this equation are selected. Ensembles for $\mathcal{F}$, T, and $\mathcal{H}$ are used to quantify uncertainty; the HadCRUT5 [18] global annual mean surface temperature T product, the F ensemble from the recent Working Group I contribution to the Intergovernmental Panel on Climate Change's Sixth Assessment Report [19], and a $\mathcal{H}$ ensemble generated from three observational ocean heat content products are used [20, 21, 22]. Figure 1 shows a regression that illustrates this process for the median radiative forcing and temperature anomaly, and the associated parameter values; heuristically the μ is chosen that makes the relationship between the x- and y-axis variables most linear (Methods), and the slope of this relationship corresponds to λ_{1970}.

Within this framework, we begin by testing the null hypothesis of a constant climate feedback from 1970–2019, i.e. $\mu = 0$. We reject this hypothesis for three reasons. When we fit our statistical model with $\mu = 0$ to the historical records, 92% of ensemble members yield curvature of the same sign in the residuals, indicating systematic behavior not captured by a constant climate feedback (Figure S1, Methods). When we compare the $\mu = 0$ model with a model with

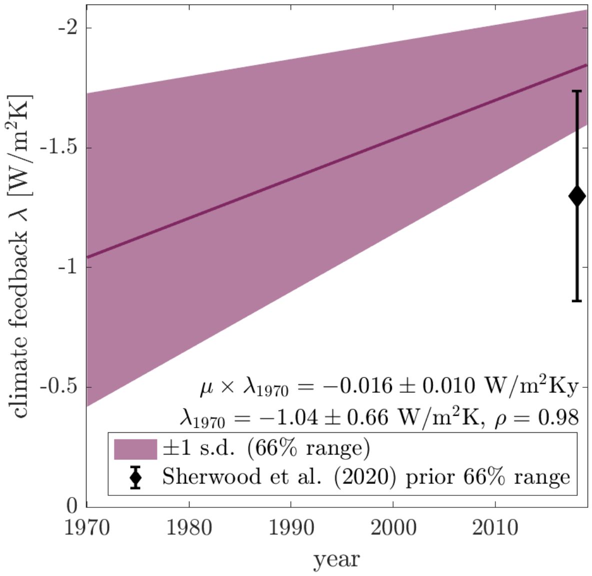

Figure 2: Median and 66% range ($\sim \pm 1$ s.d.) of the climate feedback λ. Black error bars show (time-invariant) λ mean and 66% prior range from [9] from theory and ESMs.

a nonzero μ, 91% of ensemble members yield higher Akaike Information Criterion values for the $\mu = 0$ model (Figure S1, Methods), indicating that a time-varying climate feedback describes these data better even after penalising for the additional free parameter. Finally, when μ is allowed to be nonzero, we find a decreasing climate feedback trend for 92% of ensemble members (Figure S1).

Our analysis thus suggests that λ became more negative with time (decreasing climate sensitivity) over the period 1970–2019 (i.e. $\mu > 0$). Figure 2 shows our main result; we find that λ has decreased by 0.8 ± 0.5 W/m^{2}K ($\pm$ indicates half of 66% range, or $\sim$1 standard deviation, throughout) from -1.0 ± 0.7 W/m^{2}K in 1970 to -1.8 ± 0.2 W/m^{2}K in 2019. This corresponds to an annual decrease of $\mu \times \lambda_{1970} = 0.016 \pm 0.010$ W/m^{2}K per year. The reduced uncertainty in the 2019 values is because uncertainties in μ and λ_{1970} are strongly correlated (Spearman rank correlation of 0.98). This is a large change, from a λ estimate that moves from the low end of a priori expectations (-1.3 ± 0.44 W/m^{2}K [9]; Figure 2) in 1970 to the high end in 2019. Our estimate of the change over this period of 0.8 ± 0.5 W/m^{2}K is consistent with the ESM-based quantifications of the pattern effect of 0.5 ± 0.5 W/m^{2}K [9] or 0.6 W/m^{2}K with a range of 0.3–1.0 W/m^{2}K [11]. We note that our results are consistent with the sliding window method applied to the same time series [11, 8] (Figure S2), but that this latter method has drawbacks (Methods).

One way to estimate the impact of this trend is in terms of the time taken to reach a certain warming threshold, such as those laid out in the Paris agreement [23]. To this end, we compare the time taken to reach 1.5°C and 2°C for the 1970 and 2019 values of λ. Under the idealised scenario where atmospheric CO_2 concentrations increase 1% each year [24], this results in a substantial difference in the time taken to cross these temperature thresholds; in a world with the 2019 λ value, it takes 21 ± 14 (28 ± 19) additional years to reach 1.5°C (2°C) than in a world with the 1970 value. While this is an idealised scenario and calculation, this difference demonstrates the importance of understanding and

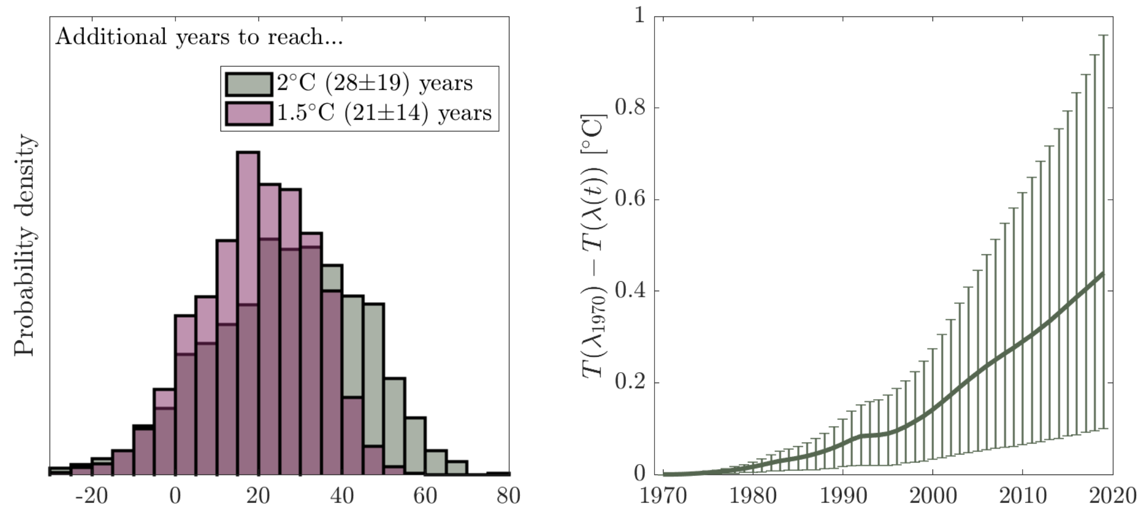

Figure 3: Left: histogram of additional years necessary to reach 1.5°C or 2°C under a 1%-per-year increase in atmospheric CO_2 concentrations using the 2019 values of λ versus the 1970 values of λ in a simple energy balance model (eq. 1). Right: Difference in T as a function of time between a scenario with observed λ trend vs. constant 1970 λ value.

predicting the evolution of λ in recent and coming years. Similarly, we estimate that if λ had remained at its 1970 value for 1970–2019, an additional ~0.4°C (66% range 0.1–1.0) warming would have occurred by 2019 (Figure 3) in addition to the ~1.2°C that has occurred since 1900.

We repeated our analysis of the historical time series with time series of model output of ensembles of historical simulations from six ESMs from CMIP6 [24] spanning a range of climate sensitivities. The ESM λ trends are either of the opposite sign to the observed trend or consistent with zero (Figure 4), because many of the climate models do not capture observed surface warming patterns [12].

On the basis of observations alone, without reference to climate models, our analysis exposes the substantial trend in the climate feedback over recent decades. Other work attributes this trend to changing patterns of sea surface warming. It remains a substantial challenge to understand this pattern effect and the evolution of climate feedback, and addressing that challenge is of paramount importance for climate projections.

References

[1] Jule G Charney et al. *Carbon dioxide and climate: a scientific assessment.* 1979.

[2] Reto Knutti, Maria AA Rugenstein, and Gabriele C Hegerl. "Beyond equilibrium climate sensitivity". In: *Nature Geoscience* 10.10 (2017), pp. 727–736.

[3] Bjorn Stevens et al. "Prospects for narrowing bounds on Earth's equilibrium climate sensitivity". In: *Earth's Future* 4.11 (2016), pp. 512–522.

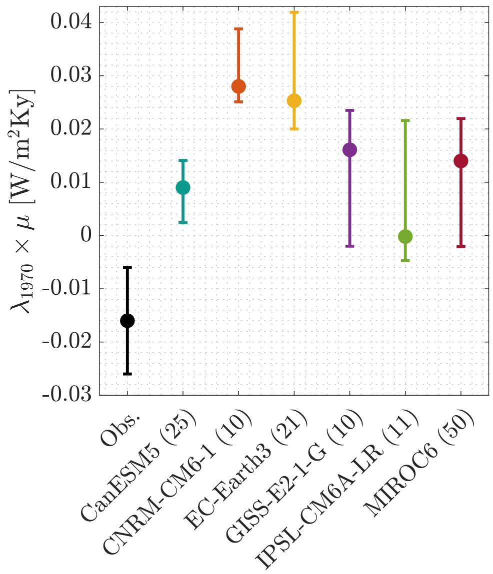

Figure 4: Median and 66% range of the trend of the climate feedback (i.e. $\mu \times \lambda_{1970}$ [W/m^{2}Ky]) for the historical records (black) and their analogs from historical simulations of six climate models (color). Ensemble size for the climate models is given in parentheses.

[4] Chen Zhou, Mark D Zelinka, and Stephen A Klein. "Impact of decadal cloud variations on the Earth's energy budget". In: *Nature Geoscience* 9.12 (2016), pp. 871–874.

[5] Yue Dong et al. "Attributing Historical and Future Evolution of Radiative Feedbacks to Regional Warming Patterns using a Green's Function Approach: The Preeminence of the Western Pacific". In: *Journal of Climate* 32.17 (2019), pp. 5471–5491. DOI: 10.1175/JCLI-D-18-0843.1. URL: https://journals.ametsoc.org/view/journals/clim/32/17/jcli-d-18-0843.1.xml.

[6] Paulo Ceppi and Jonathan M Gregory. "Relationship of tropospheric stability to climate sensitivity and Earth's observed radiation budget". In: *Proceedings of the National Academy of Sciences* 114.50 (2017), pp. 13126–13131.

[7] Timothy Andrews and Mark J Webb. "The dependence of global cloud and lapse rate feedbacks on the spatial structure of tropical Pacific warming". In: *Journal of Climate* 31.2 (2018), pp. 641–654.

[8] Jonathan M Gregory and T Andrews. "Variation in climate sensitivity and feedback parameters during the historical period". In: *Geophysical Research Letters* 43.8 (2016), pp. 3911–3920.

[9] SC Sherwood et al. "An assessment of Earth's climate sensitivity using multiple lines of evidence". In: *Reviews of Geophysics* 58.4 (2020), e2019RG000678.

[10] JM Gregory et al. "How accurately can the climate sensitivity to CO2 be estimated from historical climate change?" In: *Climate Dynamics* 54.1 (2020), pp. 129–157.

[11] Timothy Andrews et al. "Accounting for changing temperature patterns increases historical estimates of climate sensitivity". In: *Geophysical Research Letters* 45.16 (2018), pp. 8490–8499.

[12] Richard Seager et al. “Strengthening tropical Pacific zonal sea surface temperature gradient consistent with rising greenhouse gases”. In: *Nature Climate Change* 9.7 (2019), pp. 517–522.

[13] Aurélien Ribes, Said Qasmi, and Nathan P Gillett. “Making climate projections conditional on historical observations”. In: *Science Advances* 7.4 (2021), eabc0671.

[14] Katarzyna B Tokarska et al. “Past warming trend constrains future warming in CMIP6 models”. In: *Science advances* 6.12 (2020), eaaz9549.

[15] Diego Jiménez-de-la-Cuesta and Thorsten Mauritsen. “Emergent constraints on Earth’s transient and equilibrium response to doubled CO2 from post-1970s global warming”. In: *Nature Geoscience* 12.11 (2019), pp. 902–905.

[16] Femke JMM Nijsse, Peter M Cox, and Mark S Williamson. “Emergent constraints on transient climate response (TCR) and equilibrium climate sensitivity (ECS) from historical warming in CMIP5 and CMIP6 models”. In: *Earth System Dynamics* 11.3 (2020), pp. 737–750.

[17] Japan Meteorological Agency. *JMA’s global ocean heat content data.* `https://www.data.jma.go.jp/gmd/kaiyou/english/ohc/ohc_data_en.html`. [Online; accessed 7-April-2022]. 2022.

[18] Colin P Morice et al. “An updated assessment of near-surface temperature change from 1850: The HadCRUT5 data set”. In: *Journal of Geophysical Research: Atmospheres* 126.3 (2021), e2019JD032361.

[19] C Smith et al. “The earth’s energy budget, climate feedbacks, and climate sensitivity supplementary material”. In: *Climate Change* (2021).

[20] Masayoshi Ishii et al. “Accuracy of global upper ocean heat content estimation expected from present observational data sets”. In: *Sola* 13 (2017), pp. 163–167.

[21] Lijing Cheng et al. “Improved estimates of ocean heat content from 1960 to 2015”. In: *Science Advances* 3.3 (2017), e1601545.

[22] Sydney Levitus et al. “World ocean heat content and thermosteric sea level change (0–2000 m), 1955–2010”. In: *Geophysical Research Letters* 39.10 (2012).

[23] Malte Meinshausen et al. “Greenhouse-gas emission targets for limiting global warming to 2 C”. In: *Nature* 458.7242 (2009), pp. 1158–1162.

[24] Veronika Eyring et al. “Overview of the Coupled Model Intercomparison Project Phase 6 (CMIP6) experimental design and organisation.” In: *Geoscientific Model Development Discussions* 8.12 (2015).

[25] BB Cael. “Ocean heat uptake efficiency increase since 1970”. In: *Geophysical Research Letters* (2022), e2022GL100215.

[26] Alexander Otto et al. “Energy budget constraints on climate response”. In: *Nature Geoscience* 6.6 (2013), pp. 415–416.

[27] Gideon Schwarz. “Estimating the dimension of a model”. In: *The annals of statistics* (1978), pp. 461–464.

[28] Jonah Bloch-Johnson et al. "Climate sensitivity increases under higher CO_2 levels due to feedback temperature dependence". In: *Geophysical Research Letters* 48.4 (2021), e2020GL089074.

[29] BB Cael et al. "Climate nonlinearities: selection, uncertainty, projections, and damages". In: *Environmental Research Letters* (2022), p. 084025.

[30] Acknowledgements – **Funding:** Cael acknowledges support from the National Environmental Research Council through Enhancing Climate Observations, Models and Data, and the European Union's Horizon 2020 Research and Innovation Programme under grant agreement No. 820989 (project COMFORT). The work reflects only the authors' view; the European Commission and their executive agency are not responsible for any use that may be made of the information the work contains. Ceppi was supported by an Imperial College Research Fellowship and by the UK Natural Environment Research Council grants NE/T006250/1 and NE/V012045/1; Smith was supported by a NERC/IIASA Collaborative Reserach Fellowship (NE/T009381/1); Williams was supported by UK Natural Environment Research Council grant NE/T007788/1; Bloch-Johnson and Gregory were supported by the European Research Council (grant agreement No 786427, project "Couplet"). **Author contributions:** Cael led and all other authors contributed to all aspects of this work. **Competing interests:** The authors have no competing interests to declare. **Data and materials availability:** All data are available from sources cited in the text. All code and model output will be made available at github.com/bbcael and given a Zenodo DOI should this manuscript be accepted for publication.

Methods

Theory

We begin with the energy balance equation, which states that the rate of warming of the Earth's surface is proportional to its net energy imbalance at the top of the atmosphere:

$$\eta \dot{T}(t) = F(t) + \lambda(t)T(t) - H(t), \tag{1}$$

where η [W yr/m^{2}K] is the heat capacity of the layer represented by T, T is the global mean surface temperature anomaly [K], F is the radiative forcing [W/m^2], λ is the climate feedback [W/m^{2}K], and H is the heat uptake in the ocean below the layer represented by T [W/m^2]. Note that different authors use different sign conventions for λ; here, a stable climate has a negative λ. Here we are interested in the evolution of the climate feedback $\lambda(t)$. We approximate this evolution with the ansatz $\lambda(t) = \lambda_{1970}(1 + \mu t)$; for simplicity t is set to zero at 1970. We choose 1970 because both ocean heat content and global mean surface temperature increase very little prior to 1970 compared with uncertainty and interannual variability, and ocean heat content in particular before 1970 is very uncertain and sparsely observed. Inserting this ansatz and integrating both sides of this equation yields:

$$\eta T(\tau) - \eta T(1970) = \int_{1970}^{\tau} F(t)\ dt + \lambda_{1970} \int_{1970}^{\tau} (1 + \mu t) T(t)\ dt - \int_{1970}^{\tau} H(t)\ dt.$$

We then define the integrals

$$\mathcal{F}(\tau) = \int_{1970}^{\tau} F(t)\, dt, \qquad \mathcal{R}(\tau) = -\int_{1970}^{\tau} \lambda(t) T(t)\, dt, \qquad \mathcal{H}(\tau) = \eta(T(\tau) - T(1970)) + \int_{1970}^{\tau} H(t)\, dt,$$

such that $\mathcal{F}$ is the cumulative energy fluxed to the Earth's surface via radiative forcing, $\mathcal{R}$ is the cumulative energy it has fluxed back to space, and $\mathcal{H}(\tau)$ is the cumulative energy stored in the ocean and Earth's surface. These last two are combined because i) the energy stored as warming of the Earth's surface boundary layer, ηT, is predominantly stored in the upper ocean, and ii) observational records of ocean heat content cannot distinguish between the portion of energy storage in the ocean which corresponds to this ηT and energy stored below this layer, corresponding to $\int_{1970}^{\tau} H(t)\ dt$, so combining these terms is essential for comparison to observations. We can then use our ansatz and the defintion of $\mathcal{R}(\tau)$ to define

$$\mathcal{T}(\mu, \tau) = \int_{1970}^{\tau} (1 + \mu t) T(t)\, dt,$$

which after substituting in these integral terms above and rearranging yields

$$\mathcal{F}(\tau) - \mathcal{H}(\tau) = -\lambda_{1970} \mathcal{T}(\mu, \tau), \tag{2}$$

which simply states that amount of excess energy radiated back to space is equal to the excess energy added to the climate system by radiative forcing, minus the amount stored in Earth system. The term on the right hand side encodes the assumption that the climate feedback is changing with time at a constant rate. If the ansatz is valid and the correct μ is selected, this μ will capture the time-dependence of λ and the slope of the regression of the left hand side against the right hand side of the above equation will be constant in time, i.e. there will be no systematic behavior or curvature in the residuals of $\mathcal{F}(\tau) - \mathcal{H}(\tau)$ regressed against $\mathcal{T}(\mu, \tau)$; see Figure 1.

The bulk of surface warming, and hence the bulk of the concentration of warming in very negative feedback regions, occurred since 1970. Thus the diagnosed difference between λ in 1970 versus 2019 is to some extent qualitatively comparable to the pattern effect defined as difference between the climate feedback in the absence versus presence of the historical warming patterns concentrated in very negative feedback regions.

Data

For F, we use the time series ensemble (2237 members) from the Intergovernmental Panel on Climate Change's Working Group I contribution to the Sixth Assessment Report [19], which is available through 2019.

For T, we use the HadCRUT5 temperature record for global mean surface temperature because uncertainties being expressed as ensemble members makes the propagation of uncertainty straightforward when integrating in time, and the HadCRUT5 ensemble captures the uncertainty across other temperature time series [25]. T is defined as the temperature anomaly versus 1850–1900. HadCRUT5 is provided as a 200-member ensemble, described in detail in [18]; T in HadCRUT5 is a combination of surface air temperature over land and sea surface temperature elsewhere. From this ensemble a 2,237 member ensemble is generated by calculating the estimated Gaussian covariance matrix based on the ensemble and simulating 2,237 members with the same covariance properties and mean as the original ensemble. Repeating the analysis resampling directly from the 200-member ensemble had a negligible impact on the results. Note that the possible issue of Earth's climate not being well-represented as being in equilibrium in 1850–1900 is implicitly captured by the variation amongst ensemble members of $T(1970)$. On this point, we found no relationship (Pearson, Spearman, and Kendall correlations <0.1) between μ or λ_{1970} and the initial temperature $T(1970)$, indicating that any difference between the average temperature in 1850–1900 and the 'true' equilibrium temperature that T in eq. 1 is an anomaly from, does not affect our conclusions. Further to this, adding 0.08 ± 0.03 W/m^2 to F following [26] to correspond to the energy imbalance during the latter part of the 19th century had a negligible impact on the results.

For $\mathcal{H}$, we use the same method as in [25]. The Japanese Meteorologcal Agency, [20], Cheng [21], and National Centers for Environmental Information [22] ocean heat content records are provided as ocean heat content over 0-2000m. A 2,237 member ensemble is generated from these by calculating the estimated Gaussian covariance matrix from the three time-series and simulating ensemble members with the same covariance properties and mean. Years 1970 onwards are considered because ocean heat content changes are more sparsely observed and uncertain before this year and changes in both ocean heat content and temperature are very small over the years that ocean heat content data are available in a subset of these products prior to this year compared to both this uncertainty and interannual variability, indicating there is little to no signal to extract.

Primary analysis: To generate an estimate of λ_{1970} and μ for each F, T, and $\mathcal{H}$ ensemble pair, the following procedure is followed: i) sample a large range of λ_{1970}, and μ values (we sampled these at sufficiently large ranges that no parameter estimates were at the boundaries of our sampled parameter space, and at a sufficiently fine resolution in parameter space that increasing resolution by an order of magnitude did not change our results to the significant digits we report), ii) calculate the residuals in eq. 2 for these parameter values, iii) select the parameter values for which the linear regression has the lowest residual sum of squares. The linear ansatz is justified post-hoc by performing a quadratic regression of the residuals against $\mathcal{T}(\mu,\tau)$; for 99% of ensemble members the quadratic term of this regression is not significantly different from zero, and it is positive for 57% of ensemble members and negative for the other 43%.

This indicates that the assumption that λ changes constantly in time successfully captures the temporal variation in λ.

Sliding window method: Changes in λ over time have been studied in climate model simulations (particularly atmospheric simulations with prescribed sea surface temperatures) by regressing the change of global annual mean radiative response dR against surface air temperature change dT over a sliding 30-year window, e.g. [11]. We performed the same analysis on the historical time series, estimating dR as $d(F - H)$, with the standard 30-year window size. Figure S2 shows that this method agrees with our main result in Figure 2. However, it gives larger uncertainties, is dependent on the ad hoc choice of window size, can only provide estimates for the central 20 years of the time-series, over which period no significant trend in λ can be detected from either method, and use of a shorter sliding window produces estimates with large uncertainties and implausible fluctuations.

Null hypothesis: Time-evolution of λ is tested for initially by performing the primary analysis described above with $\mu = 0$. To test for systematic behavior in the residuals of the $\mu = 0$ model, a quadratic regression of Eq. 2 with $\mu = 0$ is performed for each ensemble member. For 92% of ensemble members the quadratic term is positive – – i.e. $\mathcal{F}(\tau) - \mathcal{H}(\tau)$ increases superlinearly with $\mathcal{T}(0, \tau)$ – indicating that μ is significantly positive and a necessary parameter. We demonstrate this further by comparing the models with $\mu \neq 0$ and $\mu = 0$ in terms of their Akaike Information Criterion [27] (AIC), the difference of which between two models estimates the difference in model quality. Figure S1 shows that for 91% of ensemble members, the ΔAIC values are negative, meaning the $\mu \neq 0$ model is a better description of the data even after being penalised for having an additional parameter. Similarly we see no systematic behavior in the residuals of the main regression, indicating that unlike the $\mu = 0$ case, there is no systematic behavior in the data that our $\lambda = \lambda_{1970}(1 + \mu t)$ ansatz does not capture, though of course there are multiannual fluctuations that such a simple model cannot be expected to explain. Finally, Figure S1 also shows that 92% of estimates of the trend in λ are negative, indicating that μ is significantly different from zero.

Earth system models: We perform our primary analysis on ensembles of historical simulations using six ESMs for which global F, T, and top-of-atmosphere energy imbalance are available, whose time integral is approximately equal to $\mathcal{H}$, for which we therefore use the cumulative integral noted $\mathcal{N}$. The ESMs we use are the following: CanESM5 ($n = 25$ realisations), CNRM-CM6-1 ($n = 10$), EC-Earth3 ($n = 21$), GISS-E2-1-G ($n = 10$), IPSL-CM6A-LR ($n = 11$), and MIROC6 ($n = 50$), obtained via the CMIP6 archive [24]. We append the F, T, and $\mathcal{N}$ estimates from these model realisations' Shared Socioeconomic Pathway 2-4.5 simulations for 2015–2019, because historical F is only available up until 2014, but excluding years 2015–2019 had a negligible impact on the results. We also obtained five realisations from HadGEM3-CG31-LL, one from GFDL-CM4, and three from NorESM2-LM, but these are not included in Figure 4 because only one of these nine realisations (a HadGEM3-CG31-LL realisation where $\lambda_{1970} \times \mu = +0.02$ W/m^{2}Ky) was within the range of the 2237 estimates from the observational historical ensemble, while the rest lie outside the $y-$axis range of Figure 4.

Figure 3 calculations: To estimate the difference in years taken to surpass 1.5°C or 2°C in a world that has the

1970 parameter values versus one that has the 2019 values (each as time-invariant constant values), a 1% scenario is performed using each ensemble member's i) λ_{1970} value versus ii) its climate feedback in 2019, i.e. $\lambda_{1970}(1+49\mu)$. Under the 1% scenario, atmospheric CO_2 concentrations increase by 1% per year, which under the assumption of logarithmic forcing [28] results in a linear increase in F from zero until it reaches $F_{2\times CO_2} \sim N(4.0, 0.3)$ W/m^2 after 70 years [9]. A random value of $F_{2\times CO_2}$ is sampled from $N(4.0, 0.3)$ for each ensemble member. We use the time-mean ocean heat uptake efficiency values, $\kappa = 0.58 \pm 0.08$ W/m^{2}K, estimated in a similar fashion to our primary analysis for 1970–2019 [25] in order to simulate ocean heat uptake as $H(t) = \kappa T(t)$; κ values for each ensemble member are drawn form a $N(0.58, 0.08)$ distribution. We use η values corresponding to the assumption that the surface layer represented by T has a heat capacity equal to the ocean's mixed layer, sampling from a $N(9.67, 0.8)$ J/m^{2}K distribution following the calculation in [29]. Note that this η estimate is a conservative upper limit, and that reducing the η estimate to $\sim$0 had a negligible impact on the results. Using these values for $F(t)$, η, λ, and κ, we simulate T using eq. 1 and find the year at which $T > 1.5$°C and $T > 2$°C for the 1970 and 2019 parameter values, and plot the difference between these in Figure 3. Note that this is a heuristic metric and is only intended to illustrate the potential impact of the change in λ diagnosed herein. To estimate the difference in T resulting from the trend in λ over the period 1970–2019, eq. 1 is simulated using the historical ensembles' $T(1970)$ values and F time-series, the same η and κ values as above, and either a fixed $\lambda = \lambda_{1970}$ or the time-evolving $\lambda = \lambda_{1970}(1 + \mu t)$. The right panel of figure 3 shows the difference between these two λ cases' T evolutions. This difference therefore approximates the additional warming from 1970–2019 averted due to the increase in λ over this period. Note that when the historical ensembles' H time-series are used instead of a constant κ value, this difference is larger, with a median of 0.6°C (66% range 0.1–1.4).

Supplementary figures

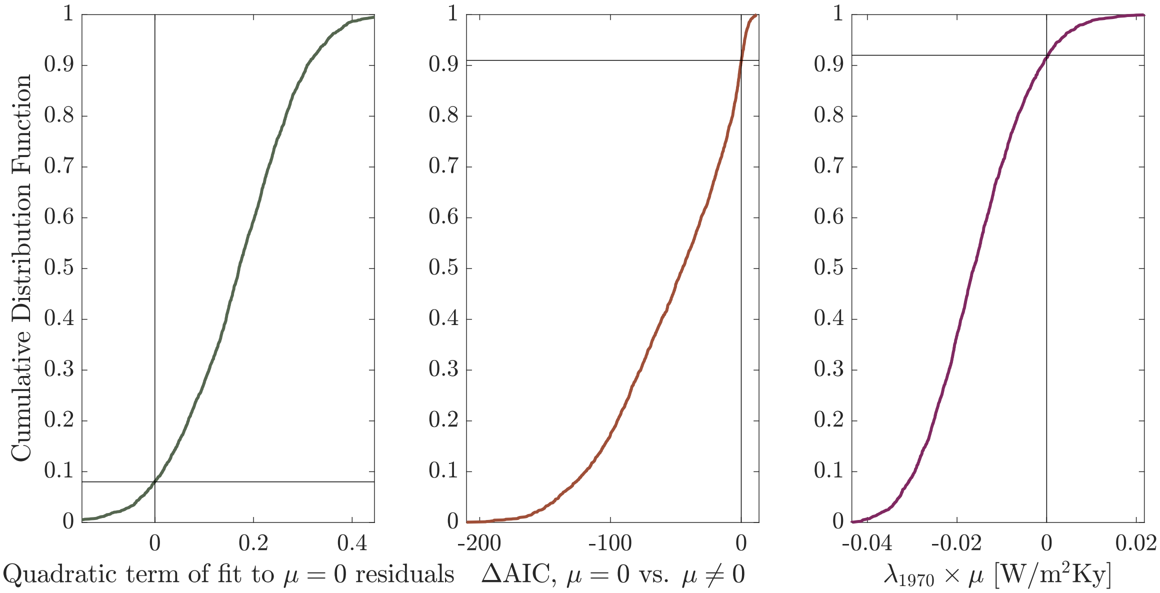

Supplementary Figure 1: Cumulative distribution functions across ensemble members of – Left: the value of the quadratic term in a quadratic polynomial fit to the residuals of the $\mu = 0$ model. Center: the difference in the Akaike Information Criterion for the ansatz used here versus a 'linear' model with a constant climate feedback. Negative ΔAIC values indicate that the ansatz used here is a better description of the historical time series. Right: the trend in λ from 1970–2019 diagnosed with the $\mu \neq 0$ model. In each case the black lines indicate the fraction of ensemble members for which the quantity on the x-axis is negative.

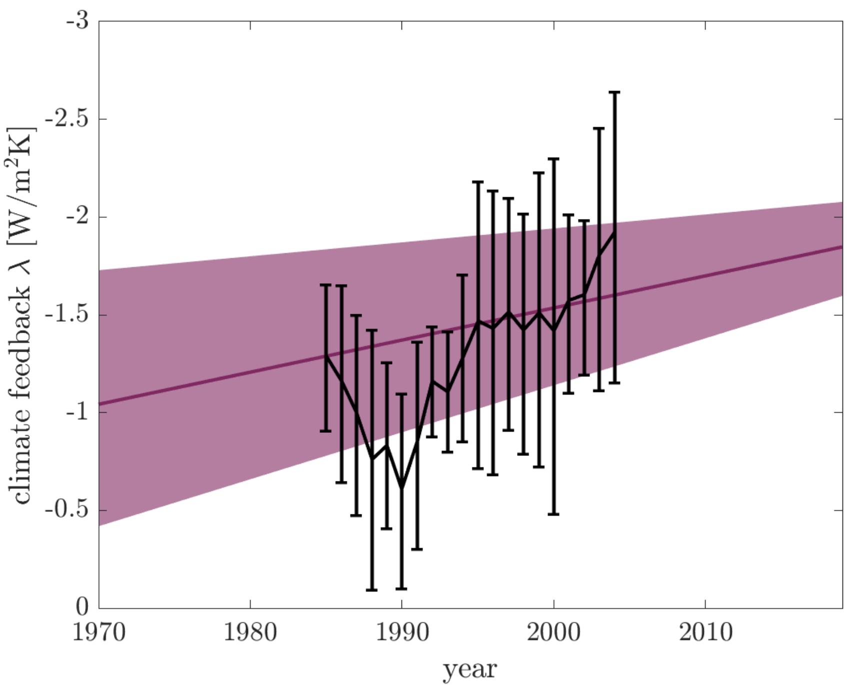

Supplementary Figure 2: As Figure 2 but with climate feedback as estimated by regression of dR against dT over a sliding window of 30 years, as in [11], superimposed. Error bars in each case represent 66% confidence interval.